中國機械工程學刊第四十一卷第二期第 121~130 頁(民國一百零九年)
Journal of the Chinese Society of Mechanical Engineers, Vol.41, No.2, pp 121~131 (2020)

Study on Rotary Ultrasonic Machining and its Predictive Model of Cutting Force on Dental Zirconia Ceramics

Kan Zheng*, Xing-Zhi Xiao**, Song Dong**, Wen-He Liao*** and Shi-Hao Liu****

Keywords： Zirconia ceramics, dental restorations, rotary ultrasonic machining, partial least squares, cutting force predictive model.

ABSTRACT

Based on the disadvantages existed in the machining of zirconia ceramic crowns, such as complicated process of sintering and difficulties in controlling shrinkage rate, the method of rotary ultrasonic machining (RUM) in sintered zirconia ceramic crowns has been proposed. The experiments of RUM have been conducted in terms of machining requirements and the failure mode of zirconia ceramic crowns. According to the influences of cutting parameters on machining qualities in different machining methods, the effect mechanism of cutting force on the labial margin edge quality and the surface damage of crowns have been revealed. Therefore, in order to control the labial margin edge quality and the surface damage effectively, a cutting force predictive model has been built based on the partial least squares (PLS) during RUM. The average error between experimental results and predictive results is only 8.23%, which indicates that the model can be applied to guide the RUM of dental zirconia ceramics for dentists.

Paper Received January 2018. Revised February, 2018, Accepted March, 2018, Author for Correspondence: Kan Zheng

* *Associate Professor, School of Mechanical Engineering, Nanjing University of Science & Technology, Nanjing, China 210094, PRC.*

** *Gradnate Student, School of Mechanical Engineering, Nanjing University of Science & Technology, Nanjing, China 210094, PRC.*

*** *Professor, School of Mechanical Engineering, Nanjing University of Science & Technology, Nanjing, China 210094, PRC.*

**** *Associate Professor, Mechanical and Electrical Engineering College, Hainan University, Haikou, China 570228, PRC.*

INTRODUCTION

Zirconia ceramics have been widely used in dental restorations due to their superior biocompatibility, sufficient chemical stability, excellent wear resistances and outstanding aesthetics (Chevalier, 2009; Hondrum,1992; Manicone,2007). During the conventional machining of all-ceramic crowns, pre-sintered ceramic blocks have been used for the contour process as the full sintered ceramic blocks are too hard and brittle for the high speed milling/grinding. Afterwards, pre-sintered zirconia ceramics crown should be sintered to get the final ceramic crowns. But the shrinkage rate could not be calculated precisely in sintering process, due to the effect of forming pressure, powder particle size, dwell time and moisture content (Inkoshi,2014). Meanwhile, intricate shape of the crowns results in difficulties on controlling the shrinkage rate. The technicians try to eliminate this shrinkage via empirical scaling the CAD model with 20%-25%. Therefore, in order to avoid the dimension error caused by sintering, the rotary ultrasonic machining technology which is considered as the most ideal and convenient method, has been introduced in the machining of dental restorations. The direct machining of full sintered zirconia ceramics could be accomplished with the assist of ultrasonic vibration. It would eliminate the crowns volume shrinkage generated in sintering as well as a time-saving process. More importantly, the introducing of this technology will change the current situation that only glass ceramics can be used in chair-side all-ceramic restoration system. The comparison of machining methods between the conventional machining and RUM is illustrated schematically in Figure 1.

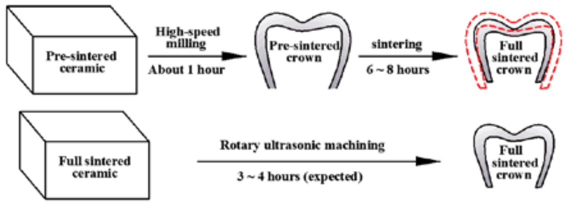

Fig. 1. Conventional machining and RUM for zirconia ceramics crowns

Recently, rotary ultrasonic machining technology has been the first choice to cut hard-and-brittle materials; Pei et al. (1993,1999) presented a material removal model of RUM in zirconia ceramics, which illuminated the relationships between the material removal rate and cutting parameters; Nath et al. (2012) conducted ultrasonic vibration assisted grinding experiments on silicon carbide ceramics, and analyzed the material removal mechanism; Yasser et al. (2012) studied RUM of alumina ceramic materials, and analyzed the trajectory of single particle and the subsurface damage mechanism; Cong (2010) and Ding (2014) contrastively analyzed the tool wear between the RUM and traditional diamond grinding (TDG) of K9 optical glass and silicon carbide, and found that the ultrasonic vibration assistance was apt to reduce the tool wear. The effect of input variables (spindle speed, feed rate and vibration amplitude) on output variables (edge chipping, cutting force and surface roughness) during RUM of glass ceramics and silicon carbide was investigated in Churi (2007,2009); Li et al. (2006) studied the influence of cutting depth, support length and preload on edge chipping of alumina ceramics via finite element method (FEM); Cheng et al (2013) carried out deep investigations on the ductile-to-brittle transition and modeled the cutting force during RUM of brittle materials. Although the processing characteristics of RUM have been studied partially, the investigation on RUM of dental zirconia ceramics is limited. Consequently, in this study, the experiments of RUM on dental zirconia ceramics have been conducted under taking the fabrication of crowns labial margin and the failure mode into consideration. The effect of cutting parameters on edge chipping and surface damage has been studied thoroughly as well as modeling of the cutting force. Hence, the influence of the cutting parameters on the cutting force during RUM of dental zirconia ceramics will be obtained, which can provide theoretical guidance for the professional staff in dental restorations.

DESIGN OF EXPERIMENTS

In order to improve the feasibility of the experiments, the straight slots are machined on the full sintered zirconia ceramics. The edges of the slot are analyzed instead of crowns labial margin, as shown in Figure 2. The workpiece is provided by Qianhuangdao aidite high-technical ceramics, CO., Ltd (the compositions and mechanical properties are shown in Table. 1 and Table. 2, respectively). It is fixed on the worktable by the paraffin with the dimension of 30mm×15mm×4mm, as illustrated in Figure 3. The machine is the rotary ultrasonic machining center (DMG Ultrasonic 20 linear, DMG, Germany), as shown in Figure 4. High-frequency ultrasonic vibration can be executed when the ultrasonic vibration system is open, whereas it is TDG mode when the system is closed. The setup mainly consists of a piezoelectric ceramic transducer, a secondary coil, an ultrasonic amplitude transformer and a tool. The main function of the setup is to transform ultrasonic electric signals to mechanical vibration, and then transmit the vibration to the end face of the tool through the amplitude transformer horn. Therefore, it would vibrate ultrasonically with microns of amplitude. Then the impacting effect and removal of the hard-and-brittle materials would be fulfilled. The tool used in the experiments is a diamond metal-bonded core tool (Schott, Germany), with the grain size of 126μm in average. Its outer diameter is 8 mm with wall thickness of 2mm. The emulsion is used as external and internal coolant during machining. The experimental variables are given in Table. 3.

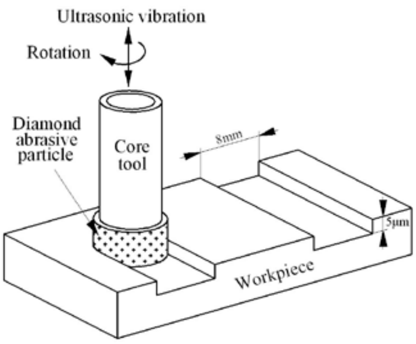

Fig. 2. Schematic illustration of RUM

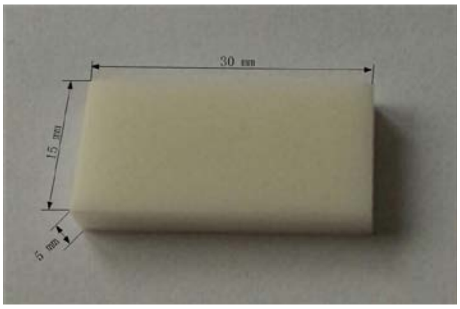

Fig. 3. Zirconis ceramic workpiece

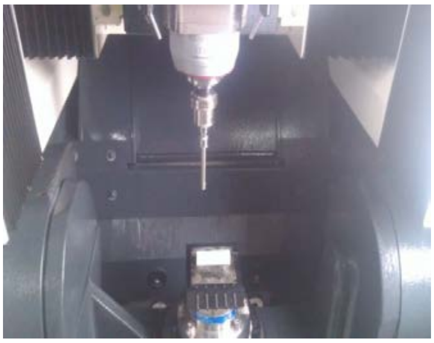

Fig. 4. Equipment for rotary ultrasonic machining

Table 1 Compositions of sintered zirconia ceramics

Compound	Content
zirconia	<96%
yttria	>4%
hafnium	>1%
alumina	<1%
silica	<0.02%

Table 2 Mechanical properties of sintered zirconia ceramics

Property	Value
Bending strength	800-1000MPa
Fracture strength	1200MPa
Vicker’s hardness/H	12GPa
Young’s modulus	210GPa
Density	6.05g/cm^3

Table 3 Experimental variables

Machining variable	Value
Spindle speed (n)	2000/4500 r/min
Feed rate (v_f)	20/40mm/min
Cutting depth (a_p)	0.005/0.015/0.020 mm
Ultrasonic amplitude (A)	4 μm
Ultrasonic vibration frequency (f)	21.3 KHz

According to the preliminary research and relative studies (Churi,2009), the effect of the ultrasonic vibration is obvious when the spindle speed reached to 2000-5000 rpm. When the spindle speed reached to a given value (such as 8000rpm and 10000rpm), the contact time between the tool and the workpiece would rise and the intermittent cutting disappears. And the effect of the ultrasonic vibration assistance would be weakened in this situation. So, the spindle speed is taken as 2000 rpm and 4500 rpm in this study. Besides, the cutting depth and feed rate are set in a low level to avoid the larger cutting force in Y direction. Otherwise it may result in the detachment of the workpiece from the worktable. The ultrasonic amplitude is determined according to the technician’s experience. The vibration frequency is detected by the sensor in the machine, and it can be read from the operation panel.

EXPERIMENTAL RESULTS AND DISCUSSION

Edge quality

The edge quality of the workpiece is an important index to evaluate its surface integrity, particularly for ceramic crowns. The machining quality of labial margin determines the accuracy of crowns. The labial margin is the external border of the crown model, which is also aligned with the gingival margin. When ceramic crowns are mounted on tooth preparations, the edge quality will affect the wear comfortability of patients and the occurrence probability of the inflammation induced by the gingival stimulation. Therefore, the edge quality of the labial margin plays a crucial role in determining the success of crowns fabrication (Stanley,1994).

The edge morphology was measured by the white light profilometer (Vyko NT9100, Veeco, USA). Figure 5a and 5b show the edge morphology of the slots machined by RUM and TDG (n=2000rpm, ap=0.015mm, vf=20 mm/min) respectively. It can be seen that the edge quality obtained from RUM is significantly better than the slot machined by TDG. The edge smoothness machined by TDG is much poorer, with continues and obvious notches. Also, the notches size in middle of the machined area is larger relatively. On the contrary, the slot machined by RUM is much better with smooth edge. The obvious edge chipping does not appear in this condition.

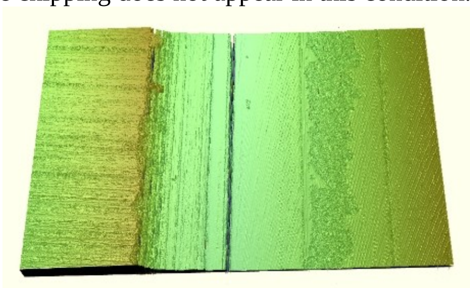

(a) Edge morphology for TDG

(b) Edge morphology for RUM

Fig. 5 Edge morphology for two machining methods

Figure 6 and Figure 7 illustrate the 3-D profiles of sintered zirconia ceramics during RUM with different cutting parameters. It can be seen from the Fig. 6 and Fig. 7 that slot edge is smooth and tidy almost without burrs when the feed rate is 20 mm/min. As the rise of feed rate, the edge quality become poor slightly, along with microscopic burrs and notches, as illustrated in Fig. 6b. Besides, the cutting depth has a greater influence on the edge quality when the spindle speed and feed rate are constant. As shown in Fig. 7b, when the cutting depth is 0.02 mm, the slot edge is not smooth and straight, and the burr can be observed in the entrance and exit of the tool. However, the condition is improved with the cutting depth decreased to 0.005 mm and 0.015 mm.

(a) v_f=20 mm/min

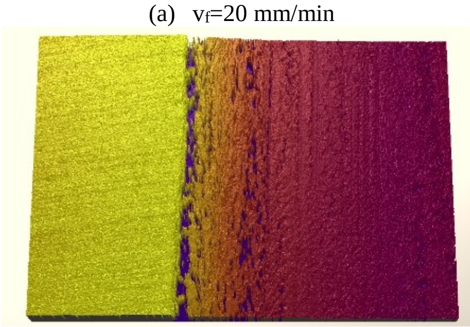

(b) v_f =40 mm/min

Fig. 6. Edge morphology for RUM with different feed rates（n=4500 rpm, a_p=0.015mm）

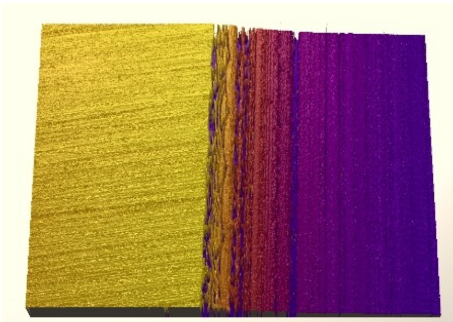

(a) a_p=0.005mm

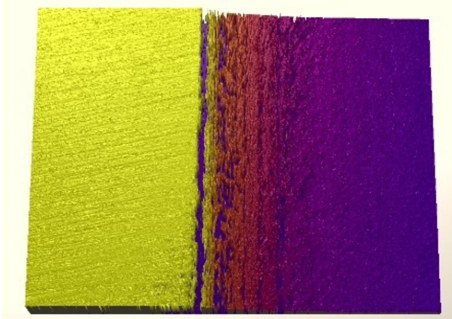

(b) a_p=0.02mm

Fig. 7 Edge morphology for RUM with different cutting depths (n=4500 rpm, v_f=40 mm/min)

Surface damage

The clinical data demonstrated that the primary failure mode of ceramic crowns is fatigue fracture, and the annual failure rate is over 3% (Zhang,2013; Chan,2013; Rekow,2005). This is affected not only by the hardness and brittleness of crowns, the bite force of the denture, but also by surface damage determined by processing technology and the thin-wall feature of the crowns. Hence, it is urgent to analyze surface damage properties of zirconia ceramics in RUM.

The surface morphology of zirconia ceramics machined by RUM is observed by the scanning electronic microscope (SEM) (JSM-6300, Jeol, Japan). Figure. 8 and Figure. 9 illustrate the surface morphology of the workpiece magnified 5000 times with different feed rate and different cutting depth, respectively. As shown from the figures, the main mode of the surface damage is fracture shedding. When the feed rate reaches to 20 mm/min (n=4000 rpm, ap=0.015 mm), there is almost no shedding on the surface, and the pit size can be ignored. However, the surface damage becomes obvious at the feed rate of 40 mm/min. In addition, as shown in Fig. 9, the shedding mode changes from small and discrete shedding to large and continues deep pit shedding as the cutting depth increases.

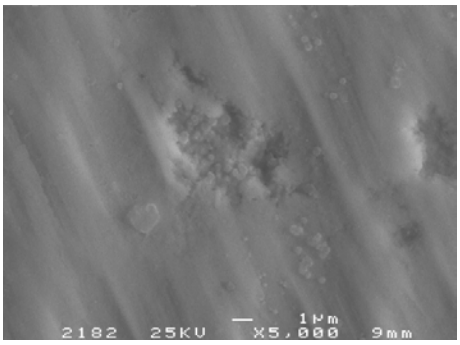

(a) v_f=20 mm/min

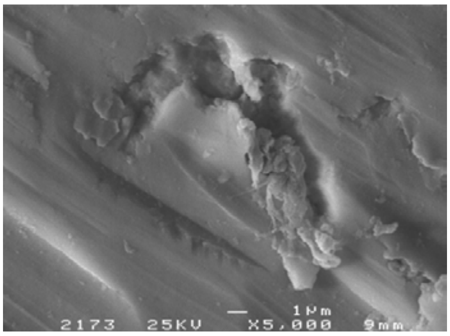

(b) v_f=40 mm/min

Fig. 8 SEM micrographs of surface morphology with different feed rates (n=4500 r/min a_p=0.015mm)

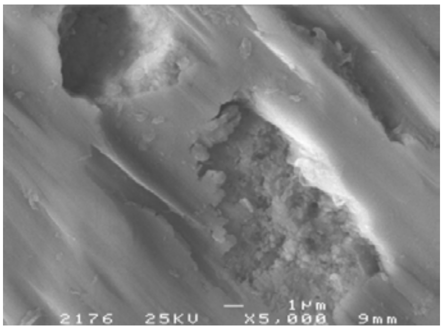

(a) a_p=0.005mm

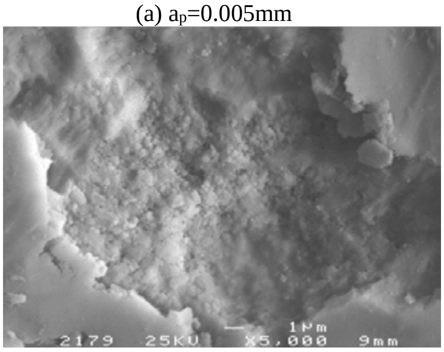

(b) a_p=0.02mm

Fig. 9 SEM micrographs of surface morphology with different cutting depths（n=4500 rpm, v_f=40 mm/min）

Discussion

1. In terms of zirconia ceramics, the breakage, cracking and material normal removal are emerged through the initiation and propagation of cracks. When slot edge is machined by diamond abrasive particles, the original cracks generate under the action of the cutting force, and then the medial-radial cracks and lateral cracks will be formed as the rise of the cutting force. When the cracks propagate towards the inside of the slot and contact with the surface, the material would be removed normally. However, when they propagate towards to the opposite direction, the chipping appears. The generation of lateral crack is illustrated in Figure.10. Its length CL and the depth CH are determined by the force loaded on the diamond particle, which are described specifically by the following equations (Marshall, 1982):

$$C_L = C_2 (\frac{1}{\tan\alpha})^{5/12} \left[\frac{E^{3/4}}{H_V K_{IC} (1-v^2)} \right]^{1/2} F_n^{5/8} \qquad (1)$$

$$C_H = C_2 (\frac{1}{\tan\alpha})^{1/3} \frac{E^{1/3}}{H_V} F_n^{1/2} \qquad (2)$$

Where H_V is the material hardness, E is the Young's modulus of the material, v is the Poisson's ratio, F_n is the load applied to the abrasive particle, C_2 is a dimensionless constant.

As shown in Fig.10a, the periodical force loaded on the diamond particles varies sinusoidally with the assistance of ultrasonic vibration. The lateral crack could not be initiated in each site due to the change of the cutting force in an ultrasonic cycle, which results in discontinuous cracks. From the position A to position C, the diamond abrasive particle is separated from the workpiece without cracks. The force loaded on the abrasive particle increases gradually from position C to position D, and the length and depth of the lateral crack will rise correspondingly based on the equations presented above. From position D to position E, the abrasive particle departs from the workpiece gradually, and the force loaded on the particle will decrease steadily which results in the decline of the length and depth of the lateral crack. Finally, the abrasive particle will separate the workpiece in position E. Thus, cracks in the zirconia ceramics cannot be coalesced easily, and the big size edge chipping cannot be formed on the edge. When the feed rate and cutting depth increase gradually, the number of the active abrasive particles and the contacting time between particles and workpiece increase correspondingly in the unit time. Then the cutting force increases, leading to the enhancement of the propagation of the cracks to some extent. Hence it results in the descent of the zirconia edge quality. For the TDG, the force loaded on the diamond particles is continuous and relative large. Hence, the steady lateral crack with a certain length and depth will generate steadily from position M to position N, which leads to the interleaving and concentration of cracks. In that case, the big size chipping will emerge along the edge.

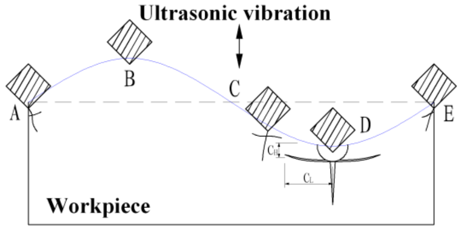

(a) RUM

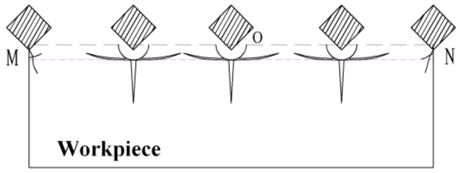

(b) TDG

Fig. 10. Generation of the lateral crack

2. The essence of RUM is a process of the material damaging and removing. Zirconia ceramics are removed with the mode of brittle fracture along with the rotary motion of the tool, due to ultrasonic impacting in the axial direction. Therefore, the number of abrasive particles taken part in hammering and grinding is increased as the rise of the feed rate and cutting depth. This results in not only the dramatic rise of the cutting force and brittle fracture of the material surface, but also the connection of fracture zones which are independent to each other originally. Consequently, the area and depth of the fracture zones become larger.

To sum up, the rise of the cutting force leads to descend of the edge quality and aggravation of the surface damage to a large extent. Therefore, how to predict and control the cutting force becomes the key factor which affects the wear comfortability and the service life of zirconia ceramic crowns.

DEVELOPMENT AND ANALYSIS OF THE CUTTING FORCE PREDICTIVE MODEL

The theoretical cutting force model of RUM has been studied extensively according to the existed research (Cheng, 2013; Wang, 2014). Acceptable results can be obtained from the theoretical model as well as different materials. However, there are many assumptions and simplifications during the modeling, such as equivalent processing of particles size, uniform distribution of abrasive particles and the materials are removed through brittle fracture, which limit the application of the model. In dental restoration field, the singleness of the material (the data form the Glidwell dental laboratory in America showed that the zirconia ceramic had accounted for 72.9% among the restorations fabricated in the laboratory) determines that an understandable and acceptable precision cutting force predictive model can be obtained for the dentists. In this study, based on the experiments conducted above, the cutting force predictive model for RUM of dental zirconia ceramics is proposed via the PLS method.

PLS method

Partial least squares regression (PLS) is a new multivariate statistical analysis method. It is suitable for analyzing the multi-correlation between different independent variables and the questions which the sample size is less than the number of the variables among multiple regression analysis. PLS is a combination of multiple regression analysis, principle component analysis, canonical correlation analysis and others basic analysis functions, which realizes the comprehensive application of various multivariate statistical analyses. It is available for handling the correlation between variables as well as the case of small sample size, which has been widely used in chemical engineering, industrial engineering and social sciences (Rosipal, 2003). In this study, PLS has been extended to construct the cutting force model in RUM of dental zirconia ceramics.

Assumed that the single dependent variable is y, the number of independent variables is $p\{x_1, x_2, x_3 \cdots, x_p\}$. n is the sample size, which forms the data tables of independent variables and dependent variable $X = (x_{ij})_{n\times p}$ and $Y = (y_i)_{n\times 1}$. These two tables are named as explanatory matrix and response variables, respectively. The basic principle of PLS is to orderly select the components $t_1, t_2, t_3 \cdots, t_h$ $(h \le p)$ whose variance $Var(t_i)$ and covariance $Cov(t_i, Y)$ is as large as possible from X according to crossover principle of effectiveness in a descending order. After that the functional relation between the Y and $x_1, x_2, x_3 \cdots, x_p$ could be obtained via building the regression equation between Y and $t_1, t_2, t_3 \cdots, t_h$. The detailed steps are shown as follows (He, 2014):

Step 1: Standardizing the independent matrix X and dependent variable Y， the standardized variable matrix E_0 and standardized column vector f_0 can be obtained as:

$$E_0 = \left(x_{ij}^*\right)_{n\times p} \qquad x_{ij}^* = x_{ij} - \overline{x}_j \tag{3}$$

$$f_0 = (y_i^*)_{n\times 1} \qquad y_i^* = y_i - \overline{y} \tag{4}$$

Where $\overline{x}_j$ and $\overline{y}$ are the average of the matrix X and dependent variable Y respectively, i. e.

$$\overline{x}_j = \frac{1}{n}\sum_{i=1}^{n} x_{ij} \qquad \overline{y} = \frac{1}{n}\sum_{i=1}^{n} y_i \tag{5}$$

Step 2: Extracting the first component t_1 from the standardized variable matrix E_0,

$$t_1 = E_0 \omega_1 \tag{6}$$

$$\omega_1 = E_0^T f_0 \tag{7}$$

Performing the regression of E_0 and f_0 on t_1:

$$E_0 = t_1 p_1^T + E_1 \tag{8}$$

$$f_0 = t_1 r_1 + f_1 \tag{9}$$

Where E_1 and f_1 is the residual matrix and vector of the regression respectively, p_1 and r_1 is described as:

$$p_1 = \frac{E_0^T t_1}{\|t_1\|_2^2} \quad r_1 = \frac{f_0^T t_1}{\|t_1\|_2^2} \tag{10}$$

Step 3: Extracting the components for E_1, E_2, f_1 and f_2 continuously to step m. The m components are named as $t_1, t_2, t_3 \cdots, t_m$, respectively. Then performing the regression of f_0 on the components:

$$f_0 = r_1 t_1 + r_2 t_2 + r_3 t_3 + \cdots r_m t_m \tag{11}$$

Substituting the above equation to it, the following equation can be obtained:

$$y = x_1 \alpha_1 + x_2 \alpha_2 + x_3 \alpha_3 + \cdots x_p \alpha_p \tag{12}$$

$$\alpha_i = \sum_{k=1}^{m} r_k \omega_{k,i}^* \quad \omega_k^* = \left[\prod_{j=1}^{k-1} (I - \omega_j p_j^T) \right] \omega_k \tag{13}$$

M is identified by the cross validation. The *ith* sample will be deleted each time among the sample sets of modeling named as $X_{(-i)}$ and $Y_{(-i)}$. Taking them as the original modeling samples, then a regression calculation will be carried out via PLS. The regression equation can be fitted with h components, and then calculate the predictive value $\hat{Y}_{h(-i)}$ which has deleted the *ith* sample point. The predictive ability of the model can be evaluated by the square of the accumulated residual and P_h:

$$P_h = \sum_{i=1}^{n} \left(Y_i - \hat{Y}_{h(-i)} \right)^2 \tag{14}$$

When the P_h is minimum, the predictive ability of the model is the best, and the component m=h

$$P(h^*) = \min_{1 \le h \le r} P_h \quad r = rank(X^T X) \tag{15}$$

Construction of the cutting force predictive model

The cutting parameters are set according to the Table 3. There are 13 experiments conducted to machine straight slots in RUM. The cutting force data is acquired by Kistler 9257 dynamometer (Kistler Instrument Corp., Amherst, NY, US) mounted between the worktable and the zirconia ceramic workpiece. Electric signals have been converted to digital signals by the A/D converter, and then read and analyzed by the Dynoware software. In this paper, the average cutting force is selected, which is the mean value of the whole cutting force in stable condition, as shown in Figure.11. The experiments design and measured results are listed in Table 4.

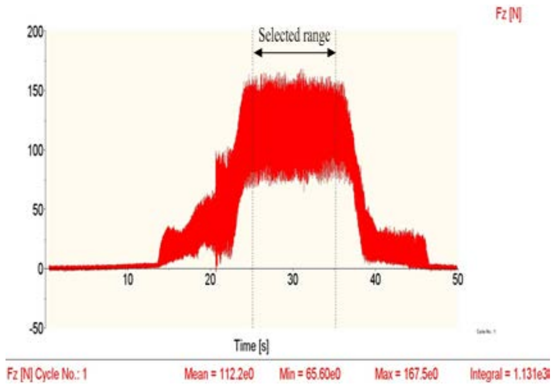

Fig. 11 Cutting force curve for second group experiment

As shown in Table 2, the value of the cutting force is large in the case of larger cutting depth and lower spindle speed, whilst the effect of feed rate on the cutting force is small. Taking the cutting parameters as independent variable matrix, the axial cutting force as dependent matrix, and then standardized respectively. Therefore the standardized variable matrix E_0 and standardized column vector f_0 can be deduced:

$$E_0 = \begin{bmatrix} -2884.62 & -0.77 & 0.00077 \\ -1384.62 & -0.77 & 0.00077 \\ 115.38 & -0.77 & 0.00077 \\ 1615.38 & -0.77 & 0.00077 \\ 115.38 & -20.77 & 0.00077 \\ 115.38 & -10.77 & 0.00077 \\ 115.38 & 9.23 & 0.00077 \\ 115.38 & -0.77 & -0.00923 \\ 115.38 & -0.77 & -0.00423 \\ 115.38 & -0.77 & 0.00577 \\ -2384.62 & 9.23 & 0.00077 \\ 615.38 & 9.23 & 0.00077 \\ 3615.38 & 9.23 & 0.00077 \end{bmatrix} \quad f_0 = \begin{bmatrix} 69.7215 \\ 11.0215 \\ -7.0485 \\ -13.0785 \\ -16.7085 \\ -12.7685 \\ -8.3185 \\ -20.7885 \\ -9.8385 \\ 6.6215 \\ 23.1215 \\ -3.0285 \\ -18.9085 \end{bmatrix} \tag{16}$$

Table 4 Design of the experiments and measured results

Serial number	Spindle speed n(r/min)	Feed rate v_f(mm/min)	Cutting depth a_p(mm)	Axial cutting force F_z(N)
1	1500	40	0.015	170.90
2	3000	40	0.015	112.20
3	4500	40	0.015	94.13
4	6000	40	0.015	88.10
5	4500	20	0.015	84.47
6	4500	30	0.015	88.41
7	4500	50	0.015	92.86
8	4500	40	0.005	80.39
9	4500	40	0.010	91.34
10	4500	40	0.020	107.80

11	2000	50	0.015	124.30
12	5000	50	0.015	98.15
13	8000	50	0.015	82.27

Table 5 Predictive values and residual sum of squares

Serial number	Experimental value	$\hat{Y}_{1(-i)}$	$\left(Y_i-\hat{Y}_{1(-i)}\right)^2$	$\hat{Y}_{2(-i)}$	$\left(Y_i-\hat{Y}_{2(-i)}\right)^2$	$\hat{Y}_{3(-i)}$	$\left(Y_i-\hat{Y}_{3(-i)}\right)^2$
1	170.90	118.54	2741.45	118.34	2762.90	118.38	2758.83
2	112.20	119.83	58.16	119.53	53.77	119.54	53.92
3	94.13	101.70	57.37	101.42	53.08	101.39	52.77
4	88.10	82.73	28.87	82.16	35.33	82.08	36.26
5	84.47	102.15	312.75	93.11	74.71	92.99	72.61
6	88.41	98.87	109.35	96.10	59.08	96.10	59.16
7	92.86	108.28	237.72	110.23	301.63	110.19	300.45
8	80.39	84.01	13.13	84.30	15.28	84.45	16.46
9	91.34	90.78	0.32	91.13	0.05	91.23	0.01
10	107.80	113.54	32.99	111.68	15.05	111.50	13.69
11	124.30	135.80	132.31	143.97	386.81	144.25	397.91
12	98.15	100.64	6.21	101.96	14.49	101.93	14.28
13	82.27	53.34	836.97	45.67	1339.47	45.57	1346.62

Table 6 Comparison between experimental and predictive results

Serial number	Experimental value	Predictive value	Relative error	Serial number	Experimental value	Predictive value	Relative error
1	170.90	136.42	20.17%	8	80.39	80.29	0.13%
2	112.20	118.75	5.84%	9	91.34	90.68	0.72%
3	94.13	101.07	7.38%	10	107.80	111.46	3.40%
4	88.10	83.40	5.34%	11	124.30	134.99	8.60%
5	84.47	92.15	9.09%	12	98.15	99.64	1.52%
6	88.41	96.61	9.28%	13	82.27	64.29	21.85%
7	92.86	105.53	13.65%				

The value of the component m is judged via cross validation, the predictive values of the axial cutting force $\hat{Y}_{h(-i)}$ and its residual sum of squares $\left(Y_i-\hat{Y}_{h(-i)}\right)^2$ were calculated as in Table 5.

According to the Table 3 and Eq.(14), the accumulated residual sum of squares P_h can be obtained as: P_1=4567.60 ; P_2=5111.64 ; P_3=5122.95 . The component m is taken as 1 because P_1 is minimum. Hence, only the regression of f_0 on t_1 needs performed.

$$\omega_1 = E_0^T f_0 = \begin{bmatrix} -370812.31 \\ 390.52 \\ 0.29 \end{bmatrix}$$

$$r_1 = \frac{f_0^T t_1}{\|t_1\|_2^2} = \begin{bmatrix} -0.011783 \\ 0.446068 \\ 2078.372495 \end{bmatrix}$$

$$y = \begin{bmatrix} x_1 & x_2 & x_3 \end{bmatrix} \begin{bmatrix} -0.011783 \\ 0.446068 \\ 2078.372495 \end{bmatrix} + 105.077674 \quad (17)$$

$$F_z = -0.011783 \times n + 0.446068 \times v_f + 2078.372495 \times a_p + 105.077674 \quad (18)$$

Analysis of the accuracy of the cutting force model

The prediction accuracy of the cutting force model affects the application feasibility of the model directly. It is also a predominant index to evaluate the reasonability of the modeling. The cross validation method has been utilized during the modeling of the cutting force, hence the sample data can be predicted and analyzed directly. The predictive values of the experiments have been calculated by the cutting force model of sintered zirconia ceramics in RUM. The relative errors of the experiments have been obtained through the comparison between experimental results and predictive results, which are illustrated in Table 6 and Figure 12.

From the Table 6 and Fig. 12, the eighth and ninth predictive results are very close to their experimental results, and the relative errors are 0.13% and 0.72% respectively. In contrast, the first and thirteenth predictive errors account for 20% nearly. In the first experiment, the spindle speed is 1500rpm, while it is 8000rpm in the thirteenth experiment. They are just in the two extremes of the spindle speed used in this experimental design. When the spindle speed is low (1500rpm), the sharp increase in feed per revolution causes a significant increase in cutting force. Conversely, the cutting process becomes lighter in high spindle speed, and the cutting force decreases significantly. So the force data in these two experiments appears significant deviation compared to other experiments, which results in poor prediction accuracy of these two results (more than 20%). Obviously, spindle speed significant effected the model prediction accuracy. Additional, PLS method could identify singularity actively, and aggregate the others. It also caused the accuracy error between them.

The predictive results of other groups are relative reasonable, and the average relative error is only 8.23%, which shows a good prediction accuracy. Meanwhile, the cross validation has been used to determine the number of components during the modeling of the cutting force, which confirmed that the predictive results of the model had a good generalization ability. Therefore, the model is reasonable and reliable in RUM of zirconia ceramic crowns. It can provide theoretical guidance for professional staff in dental restorations field.

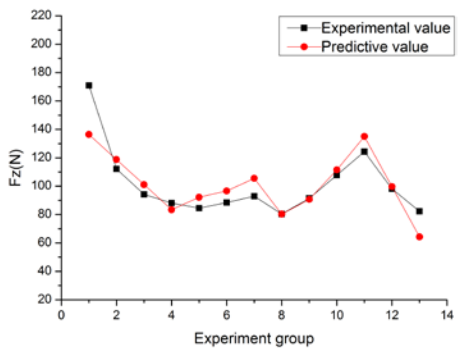

Fig. 12 Comparison between experimental values and predictive values

CONCLUSIONS

With the improvement of the living standard, people are paying more attention to the wear comfortability, service life and aesthetics of crowns. Therefore, how to ensure the machining accuracy, improve the edge quality of the labial margin and control the surface damage of the crowns becomes the central issue. Consequently, the experiments have been conducted in RUM of full sintered zirconia ceramics based on the advantages of rotary ultrasonic machining hard-and-brittle materials. The effect of cutting parameters on edge quality and surface damage has been analyzed, and the cutting force predictive model in RUM of dental zirconia ceramics has been proposed. The conclusions can be drawn as follows:

1. The edge quality of zirconia ceramics in RUM is obvious better than in TDG under same input variables. The rise of the cutting depth and feed rate leads to the decline of the edge quality of ceramics, and the effect of the cutting depth is significant.

2. The primary damage mode of zirconia ceramics during RUM is fracture shedding. The increasing of the spindle speed and feed rate results in the aggravation of the impact effect of active abrasive particles, which causes the rise of the area and depth of the fracture zone.

3. The number of the active abrasive particles increases with the rise of the cutting depth and feed rate during RUM, which improved the cutting force and aggravated the brittle fracture of the surface. Hence, the rise of the cutting force is the primary factor which results in the decrease of the edge quality and aggravation of the surface damage.

4. The predictive model of the cutting force during RUM of dental zirconia ceramics reflects high prediction accuracy. It is available for the dentists to obtain the predictive value of the cutting force quickly and accurately before the manufacture of the crowns and other restorations. Although the feasibility of the RUM in dental zirconia ceramics is still in the theoretical stage, this study can provide some guidance for the further research on cutting force control and parameters optimization.

ACKNOWLEDGMENT

This research was financially supported by the National Nature Science Foundation of China (Grant No.51675284 and 51305206).

REFERENCES

Chevalier, J., and Gremillard, L., "Ceramics for medical applications: a picture for the next 20 years," J. Eur. Ceram. Soc., Vol. **29**, pp. 1245-1255(2009).

Hondrum, S. O., "A review of strength properties of dental ceramics," J. Prosthet. Dent., Vol.**67**, pp.859–865(1992).

Manicone, P. F., Rossi, I. P., and Raffaelli, L., "An overview of zirconia ceramics:basic properties and clinical applications," Dent., Vol.35, NO.11, pp.819-826(2007).

Inkoshi, M., Zhang, F., and Munck, J. D., "Influence of sintering conditions on low-temperature degradation of dental zirconia," Dental. materials., Vol.30, No.6, pp.669-678(2014).

Pei, Z. J., and Ferreira, P. M., "An Experimental Investigation of Rotary Ultrasonic Face Milling," International. Journal. of Machine. Tools &

Manufacture., vol.39, pp.1327–1344(1999).
Pei, Z. J., Prabhakar, D., and Ferreira, P. M., “A mechanistic approach to the prediction of material removal rates in rotary ultrasonic machining,” Manufacturing. Science and engineering., Vol.64, pp.771-784(1993).
Nath, C., Lim, G. C., and Zheng, H. Y., “Influence of the material removal mechanisms on hole integrity in ultrasonic machining of structural ceramics,” Ultrasonics., Vol.52,No.5, pp.605-613(2012).
Yasser, A., Cong, W. L., and Matthew, R. S., “Rotary Ultrasonic Machining of Alumina Dental Ceramics: A Preliminary Experimental Study on Surface and Subsurface Damages,” Journal of Manufacturing Science and Engineering., Vol.134, pp.1-5(2012).
Gong, H., Fang, F. Z., and Xu, X. T., “ Kinematic view of tool life in rotary ultrasonic side milling of hard and brittle materials,” International Journal of Machine Tools & Manufacture., Vol.50, pp.303-307(2010).
Ding, K., Fu,Y. C., and Su, H. H., “Wear of diamond grinding wheel in ultrasonic vibration-assisted grinding of silicon carbide,” Int. .J Adv. Manuf. Technol., Vol.71, No.9-12, pp.1929-1938(2014).
Churi, N. J., Pei, Z. J., “Shorter D.C. Rotary Ultrasonic Machining of Dental Ceramics,” Int.J. Machining and Machinability of Materials., Vol.6, No.3,, pp.270-284(2009).
Churi, N. J., Pei, Z. J.,and Treadwell, C., “Rotary ultrasonic machining of silicon carbide: designed experiments,” International journal of manufacturing technology and management, Vol.12,No.3, pp.284-298(2007).
Z, C. Li, Liang-Wu., and Cai, Z, J. Pei., “Edge-chapping reduction in rotary ultrasonic machining of ceramics:Finite element analysis and experimental verification,” International Journal of Machine Tools & Manufacture,Vol.46,No.12, pp.1469-1477(2006).
Cheng, L.Z., Ping, F.F., and Jian, F.Z., “Ultrasonic Vibration-assisted Scratch-induced Characteristics of C-plane Sapphire with a Spherical Indenter,” International Journal of Machine Tools and Manufacture, Vol.64, pp. 38-48(2013).
Stanley, G. V., Mysore, K.P., and John, R.A., “Effect of ultrasonic cleaning and air polishing on porcelain labial margin restorations,” Journal of prosthetic dentistry, Vol.71, No.5, pp.447-452(1994).
Zhang, Y., Sailer, I., and Lawn, B.R., “Fatigue of dental ceramics,” Journal of dentistry, Vol.41, No.12, pp.1135-1147(2013).
Chan, R.N., Stoner, B.R,Thompson J Y, etc. Fracture toughness improvements of dental ceramic through use of yttria-stabilized zirconia (YSZ) thin-film coatings[J]. Dental materials,2013,29():881-887.
Rekow, E.D., and Thompson, V.P. “Near-Surface Damage—A Persistent Problem in Crowns Obtained by Computer-Aided Design and Manufacturing.Proc,” Inst. Mech. Eng., Part H: J. Eng. Med., Vol.219, No. 4, pp.233-243(2005).
Marshall, D.B., Lawn, B.R., and Evans, A.G., “Elastic/plastic indentation damage in ceramics: the lateral crack system,” Journal of the American Ceramic Society,Vol.65, pp.561–566(1982).
Wang, C.L., Pei, Z.J, and Sun, X., “Rotary ultrasonic machining of CFRP: A mechanistic predictive model for cutting force,” Ultrasonics., Vol.54, No.2, pp.663-675(2014).
Rosipal, R., “Kernel partial least squares for nonlinear regression and discrimination,” Neural. Network World, Vol.13, No.3, 291-300(2013).
He, K.F., Qian, W.Q., and Zhang, Y., “Application of partial least squares regression method in modeling of aerodynamic data,” Journal of Astronautics, Vol. 35, No.3, pp.277-282(2014).

牙科氧化鋯陶瓷的旋轉超聲加工及其切削力預測模型研究

鄭侃 肖行誌 廖文和 董松
南京理工大學機械工程學院

劉世豪
海南大學機電工程學院

摘 要

考慮到氧化鋯陶瓷牙冠現有制造工藝存在二次燒結加工工藝復雜、收縮率難以控制等問題，提出了采用旋轉超聲加工完全燒結氧化鋯陶瓷牙冠的方法。針對氧化鋯陶瓷牙冠的制造要求和失效模式，開展了旋轉超聲加工實驗研究。通過對比不同加工方法和切削參數對氧化鋯陶瓷工件加工質量的影響程度，闡明了超聲振動輔助下，切削力對牙冠頸緣線棱邊質量及表面損傷的作用機理。因此，為了實現對牙冠頸緣線棱邊質量和加工表面損傷的控制，以 13 組實驗數據為樣本，建立了壹種基於偏最小二乘法的旋轉超聲加工牙科氧化鋯陶瓷的切削力預測模型。將切削力的預測值與實驗值進行對比表明，所構建的切削力預測模型的平均誤差僅為 8.23%，體現了良好的預測精度。